Numerical modeling of turbulence mixed convection heat transfer in air filled enclosures by finite volume method

Mohammad Reza Safaei[1*], Marjan goodarzi[1] and Mohammadali Mohammadi[2]
[1]Mashhad Branch, Islamic Azad University, Mashhad, Iran
[2]University Putra Malaysia, Serdang, Malaysia

ABSTRACT
In the present study, first the turbulent natural convection and then laminar mixed convection of air flow was solved in a room and the calculated outcomes are compared with results of other scientists and after showing validation of calculations, aforementioned flow is solved as a turbulent mixed convection flow, using the valid turbulence models Standard k–ε, RNG k–ε and RSM.

To solve governing differential equations for this flow, finite volume method was used. This method is a specific case of residual weighting method. The results show that at high Richardson Numbers, the flow is rather stationary at the center of the enclosure. Moreover, it is distinguished that when Richardson Number increases the maximum of local Nusselt decreases. Therefore, it can be said that less number of Richardson Number, more rate of heat transfer.

Keywords: Mixed Convection Heat Transfer, Turbulence Models, Nusselt Number, Turbulent Kinetic Energy, Reynolds Stress.

1. INTRODUCTION

Mixed convection heat transfer is a phenomenon in which both natural and forced convections happen. Mixed convection heat transfer takes place either when buoyancy effect matters in a forced flow or when there are sizable effects of forced flow in a buoyancy flow. Dimensionless numbers to determine this type of flow are as follows: Grashof Number ($\mathrm{Gr} = g.\beta.\Delta T.\mathrm{L}^3/\nu^2$), Reynolds Number ($\mathrm{Re} = \rho.v.\mathrm{l}/\mu$), Rayleigh Number ($\mathrm{Ra} = \mathrm{Gr.Pr}$), Prandtl Number ($\mathrm{Pr} = C_p.\mu/\mathrm{K}$), and Richardson Number (Ri). If you devide natural convection effect by forced convection effect, it yields to Richardson number and it is written as such: $\mathrm{Ri} = \mathrm{Gr}/\mathrm{Re}^2$. When it comes to limits and we have $\mathrm{Ri}\to 0$ or $\mathrm{Ri}\to\infty$, forced convection and natural convection become dominant heat transfers respectively [Bejan [1]].

Mixed convection heat transfer is a fundamentally significant heat transfer mechanism that occurs in selection industrial and technological applications.

In the recent years, wide and practical usages of mixed convection heat transfer in areas such as designing solar collectors, double-layer glasses, building insulations, cooling electronic parts and have attracted many scientists in studying it.

*Corresponding author. Tel.: +989151022063; E-mail address: CFD_Safaiy@yahoo.com

Fluid flow and heat transfer in rectangular or square cavities driven have been studied extensively in the literature. A review shows that there are two kinds of studies:

One way includes the entry of hot (or cold) fluid from one side, passing isothermal walls, and exit from the other side. In this case, we could evaluate and compare the forced convection effect caused by the entry and exit of the fluid. Some scientists have applied thermal flux on the way fluid passes through the channel and then, they studied the effects of it. Among the studies, we can mention the ones done by Rahman et al. [2], Saha et al. [3] and Saha et al. [4]. Another method to create mixed convections is to move enclosure walls in presence of hot (cold) fluid inside the enclosure. This creates shear stresses and provides thermal and hydrodynamic boundary layers in the fluid inside the enclosure, and eventually creates forced convection in it. Numerous studies have been conducted in this field so far. We can mention the study done by Ghasemi & Aminossadati [5] as an instance. They have studied heat transfer of natural convection in an inclined square enclosure that had two insulated vertical walls and two horizontal walls with different temperatures with using finite volume method. They studied pure water and CuO-water with $0.01 \leq \Phi \leq 0.04$. They varied Rayleigh number between 10^3 and 10^7 and inclination angle between 0 Degrees to 90 Degrees and studied the impact of these factors on heat transfer and fluid flow in the enclosure. They found that in low Rayleigh numbers - which heat transfer, is in a conduction way — flow pattern and temperature in the inclination angles range of 30 degrees to 90 degrees is similar. However, for Rayleigh numbers bigger than 10^5, temperature and flow pattern is different in inclination angle = 0 degree from other inclination angles.

Basak et al. [6] Studied the mixed convection flow inside a square enclosure with left and right cold walls, insulated moving upper wall, and fixed lower hot wall by using finite element method. They suggested that by increasing Gr, when Pr and Re are fixed, recirculation power would improve.

In year 2007, Khanafer et al. [7] numerically studied unsteady mixed convection of a simple fluid in a sinusoidal lid-sliding cavity. Their study showed that Grashof and Reynolds numbers had an undeniable impact on nature and structure of the flow.

It is undeniable that the advancement in different sciences in the last decade has resulted in much subtle laboratory measuring tools and it is true that using of modern methods like parallel processing has enabled us to efficiently use numerical analysis methods. Yet analysis of turbulent flows inside the enclosure is still a challenging topic in fluid mechanics. That is because in experimental situation, it is too difficult to reach ideal adiabatic wall condition. It is at the same time difficult to measure low speeds in enclosure boundary layers through using present sensors and probes. Even numerically, although numerical methods like DES, LES, and DNS have been subject to dramatic advancements, it is still nearly impossible to predict the stratification in the core of the enclosure. Non-linearity and coupling of the predominant equations have contributed into making the calculations complicated and time consuming. That is while in designing large enclosures, Rayleigh number is usually large, and so the flow nature is turbulent [Goshayeshi and safaei [8]]. The complexity of calculations in mixed convection has made scientists to just study natural convection, among which we can mention the studies Bessaih and Kadja [9], Ampofo [10], Salat et al. [11], Xaman et al. [12] and Aounallah et al. [13]. In 2000, Tian and Karayiannis [14] started an experimental study in South Bank University that was followed by Ampofo and Karayiannis [15]. Data in this work were experimental benchmark data of natural convection flow inside a square enclosure, and were used for other studies. Whereas Peng and Davidson [16] studied the mentioned flow by using LES, and Omri and Galanis [17] used the SST k-ω to study this flow. Hsieh and Lien [18] used turbulence models of steady RANS like Low-Re k-ε, and

numerically analyzed the works done by Betts and Bokhari [19] and Tian and Karayiannis [14]. In the present work, turbulent natural convection inside square and rectangular enclosures is modeled first, and the results have been compared with the studies Betts and Bokhari [19] and Tian and Karayiannis [14], Ampofo and Karayiannis [15], Peng and Davidson [16], Omri and Galanis [17] and Hsieh and Lien [18]. After the calculations being valid, first the Laminar mixed convection flow is solved in the square enclosure, in comparison with Basak et al. [6] and eventually turbulence mixed convection in square enclosure is modeled for the first time in all of the world, by using turbulence models like Standard k-ε, RNG k-ε and RSM.

2. PROBLEM FORMULATION

For modeling the investigated flow, continuity, we solve momentum, energy, and turbulence equations. The properties have been considered fixed of course. Density is calculated vertically by using variable density parameter for ΔT>30¡C and Boussinesq approximation for ΔT<30¡C. The governing equations are as follow:

Continuity equation:

$$\frac{\partial u}{\partial x}+\frac{\partial v}{\partial y}=0 \tag{1}$$

Momentum equations in X and Y Direction:

$$\frac{\partial u}{\partial t}+u\frac{\partial u}{\partial x}+v\frac{\partial u}{\partial y}=-\frac{1}{\rho}\frac{\partial p}{\partial x}+\frac{\partial}{\partial x}(\upsilon+\upsilon_t)\left(2\frac{\partial u}{\partial x}\right)+\frac{\partial}{\partial y}(\upsilon+\upsilon_t)\left(\frac{\partial u}{\partial y}+\frac{\partial v}{\partial x}\right) \tag{2}$$

$$\frac{\partial v}{\partial t}+u\frac{\partial v}{\partial x}+v\frac{\partial v}{\partial y}=-\frac{1}{\rho}\frac{\partial p}{\partial x}+g\beta(T-T_m)+\frac{\partial}{\partial y}(\upsilon+\upsilon_t)\left(2\frac{\partial v}{\partial y}\right)+\frac{\partial}{\partial x}(\upsilon+\upsilon_t)\left(\frac{\partial v}{\partial x}+\frac{\partial u}{\partial y}\right) \tag{3}$$

Energy equation:

$$\frac{\partial T}{\partial t}+u\frac{\partial T}{\partial x}+v\frac{\partial T}{\partial y}=\frac{\partial}{\partial x}\left(\frac{\nu}{\mathrm{Pr}}+\frac{\nu_t}{\sigma_T}\right)\frac{\partial T}{\partial x}+\frac{\partial}{\partial y}\left(\frac{\nu}{\mathrm{Pr}}+\frac{\nu_t}{\sigma_T}\right)\frac{\partial T}{\partial y} \tag{4}$$

Now for k-ε model, we will have:

Turbulent kinetic energy transport equation:

$$\frac{\partial k}{\partial t}+u\frac{\partial k}{\partial x}+v\frac{\partial k}{\partial y}=\frac{\partial}{\partial x}\left(\upsilon+\frac{\upsilon_t}{\sigma_k}\right)\frac{\partial k}{\partial x}+\frac{\partial}{\partial y}\left(\upsilon+\frac{\upsilon_t}{\sigma_k}\right)\frac{\partial k}{\partial y}+P_k+G_k-\varepsilon \tag{5}$$

Dissipation of turbulent kinetic energy transport equation:

$$\frac{\partial \varepsilon}{\partial t}+u\frac{\partial \varepsilon}{\partial x}+v\frac{\partial \varepsilon}{\partial y}=\frac{\partial}{\partial x}\left(\upsilon+\frac{\upsilon_t}{\sigma_\varepsilon}\right)\frac{\partial \varepsilon}{\partial x}+\frac{\partial}{\partial y}\left(\upsilon+\frac{\upsilon_t}{\sigma_\varepsilon}\right)\frac{\partial \varepsilon}{\partial y}+C_1\frac{\varepsilon}{k}P_k+C_2\frac{\varepsilon^2}{k}+C_3\frac{\varepsilon}{k}G_k-R_\varepsilon \tag{6}$$

The eddy viscosity obtained from Prandtl- Kolomogorov relation:

$$\upsilon_t=C_\mu f_\mu\frac{k^2}{\varepsilon} \tag{7}$$

The stress production term, P_k, is modeled by:

$$P_k = \upsilon_t \left[2\left(\frac{\partial u}{\partial x}\right)^2 + 2\left(\frac{\partial v}{\partial x}\right)^2 + \left(\frac{\partial u}{\partial y} + \frac{\partial v}{\partial y}\right)^2 \right] \tag{8}$$

The buoyancy term, G_k, is defined by:

$$G_k = -g\beta \frac{\upsilon_t}{\sigma_t} \frac{\partial T}{\partial y} \tag{9}$$

We will also have the following for RNG k-ε:

$$R_\varepsilon = \frac{C_\mu \rho \eta^3 \left(1 - \frac{\eta}{\eta_0}\right)}{1 + \beta \eta^3} \frac{\varepsilon^2}{k} \tag{10}$$

That:

$$\eta = \frac{Sk}{\varepsilon} \tag{11}$$

The main difference between standard k-ε and RNG k-ε methods is in the ε equation, such that we can say the RNG k-ε model is very same to standard k-ε model, but analytical formulas for turbulent Prandtl Numbers have been improved. This is while these values in standard k-ε model are gained experimentally.

For RSM model, the turbulence equations are as follows:

Reynolds stress transport equations:

$$\frac{D}{Dt}\left(\overline{u_i' u_j'}\right) = \frac{\partial\left(d_{ijk}\right)}{\partial x_k} + P_{ij} + G_{ij} + \phi_{ij} - \varepsilon_{ij} \tag{12}$$

That:

$$\frac{D}{Dt}\left(\overline{u_i' u_j'}\right) = \frac{\partial\left(\overline{u_i' u_j'}\right)}{\partial t} + \bar{u}_k \frac{\partial\left(\overline{u_i' u_j'}\right)}{\partial x_k}: \qquad \text{Advection (By Mean Flow)}$$

$$d_{ijk} = v \frac{\partial\left(\overline{u_u' u_j'}\right)}{\partial x_k} - \overline{\frac{P'}{\rho}\left(u_i' \delta_{jk} + u_j' \delta_{ik}\right)} - \overline{u_i' u_j' u_k'}: \qquad \text{Diffusion}$$

$$P_{ij} = -\left[\left(\overline{u_i' u_k'}\right)\frac{\partial \bar{u}_j}{\partial x_k} + \left(\overline{u_j' u_k'}\right)\frac{\partial \bar{u}_i}{\partial x_k}\right]: \qquad \text{Production (By Mean Strain)}$$

$$G_{ij} = \left(\overline{u_i' f_j' + u_j' f_i'}\right): \qquad \text{Production (By Body Force)}$$

$$\phi_{ij} = \overline{\frac{P'}{\rho}\left(\frac{\partial u_i'}{\partial x_j} + \frac{\partial u_j'}{\partial x_i}\right)} = \overline{\frac{2P'}{\rho} S_{ij}}: \qquad \text{Pressure-Strain Correlation}$$

$$\varepsilon_{ij} = 2\nu\overline{\frac{\partial u_i'}{\partial x_k}\frac{\partial u_j'}{\partial x_k}}: \qquad \text{Dissipation}$$

Turbulent kinetic energy transport equation:

$$\frac{Dk}{Dt} = \frac{\partial d_i^{(k)}}{\partial x_i} + P^{(k)} + G^{(k)} - \varepsilon \tag{13}$$

Except the terms Convection and Production in Reynolds stress transport equation, all the other terms have contributed in introducing a series of correlations, which have to be identified according to some known and unknown quantities, so that the equation system can be configured.

Diffusion term:

$$-\overline{u_i' u_j' u_k'} = C_S \frac{k}{\varepsilon}\overline{u_k' u_l'}\frac{\partial \overline{u_i' u_j'}}{\partial x_l} \tag{14}$$

Redistribution term:

$$\phi_{ij} = \phi_{ij}^{(1)} + \phi_{ij}^{(2)} + \phi_{ij}^{(w)} \tag{15}$$

That:

$$\begin{aligned}
\phi_{ij}^{(1)} &= -C_1 \frac{\varepsilon}{k}\left(\overline{u_i' u_j'} - \frac{2}{3}k\delta_{ij}\right) \\
\phi_{ij}^{(2)} &= -C_2\left(P_{ij} - \frac{1}{3}P_{kk}\delta_{ij}\right) \\
\phi_{ij}^{(w)} &= \left(\tilde{\phi}_{kl} n_k n_l \delta_{ij} - \frac{3}{2}\tilde{\phi}_{ik} n_j n_k - \frac{3}{2}\tilde{\phi}_{jk} n_i n_k\right)\psi \\
\tilde{\phi}_{ij} &= -C_1^{(w)} \frac{\varepsilon}{k}\overline{u_i' u_j'} + C_2^{(w)}\phi_{ij}^{(2)}
\end{aligned} \tag{16}$$

$$\psi = \frac{k^{\frac{3}{2}} / \varepsilon}{C_3 y_n}$$

y_n is the distance from the wall. The role of terms $\Phi_{ij}^{(2)}$, $\Phi_{ij}^{(1)}$ is to return isotropy (or terminating anisotropic flow with distributing kinetic energy of Reynolds huge stresses among the stresses of smaller size). The terms $\Phi_{ij}^{(1)}$ and $\Phi_{ij}^{(2)}$ are called return to isotropy and isotropization of production , respectively. The term $\Phi_{ij}^{(w)}$ is named as wall reflection term .

For Dissipation term, we have:

$$\varepsilon_{ij} = \frac{2}{3}\delta_{ij}\varepsilon \tag{17}$$

The constants in the above relations have been presented in table 1 for RNG k-ε, table 2 for standard k-ε, and in table 3 for RSM models [Safaei [20]].

In order to solve differential equations that govern on the flow, we will use finite volume method, which is explained with details by Patankar [21] and Goshayeshi, Safaei and Maghmoomi [22]. This method is a specific case of residual weighting methods. In this approach, the computational field is divided to some control volumes in a way that a control volume surrounds each node and control volumes have no volumes in common. The differential equation is then integrated on each control volume. Profiles in pieces which show changes (of a certain quantity like temperature, velocity, etc.) among the nodes, are used to calculate the integrals. The result is discretization equation, which includes quantities for a group of nodes.

In this way, the answer is always probed on the grid-points and interpolation formulas (piecewise profiles) are necessary to calculate integrals and used within our calculations. When we get discretized equations, these assumption profiles can be forgotten and we have complete freedom to adopt various assumptions for these profiles. The advantage of this method is high accuracy and exact integral balances even in coarse grids [Patankar [21]].

Table 1 Coefficients for RNG k-ε turbulent model

C_μ	σ_k	σ_ε	C_1	C_2	η_0	β	K
0.0845	1	1.3	1.42	1.68	4.38	0.012	0.41

Table 2 Coefficients for Standard k-ε turbulent model

C_μ	σ_k	σ_ε	C_1	C_2
0.0845	1	1.3	1.42	1.68

Table 3 Coefficients for RSM turbulent model

$c_2^{(w)}$	$c_1^{(w)}$	C_s	C_1	C_2	C_3
0.3	0.5	0.22	1.8	0.6	2.5

3. RESULTS

3.1. MESH INDEPENDENCY

Meshes that designed to cover control volumes, are square meshes provided on physical domain with different distances in order to reach independence. The mentioned mesh-independence for each turbulence model and any different Ri has been separately calculated. Table 4 shows some meshes used in this study.

3.2. EVALUATION OF TURBULENT NATURAL CONVECTION FLOW INSIDE THE ENCLOSURE

In order to demonstrate the accuracy of calculations, first of all, natural convection heat transfer is solved in rectangular and square enclosures studied by other scientists like Betts and Bokhari [19] and Tian and Karayiannis [14], Ampofo and Karayiannis [15], Peng and Davidson [16], Omri and Galanis [17] and Hsieh and Lien [18].

After validating the results (see figures 1 and 2) with other scientists conclusions, it can be concluded that the procedure of solving the problem in this study is correct. Moreover, the flow is solved inside the enclosure assuming mixed convection conditions.

3.3. EVALUATION OF LAMINAR MIXED CONVECTION FLOW INSIDE A SQUARE ENCLOSURE

In order to compare with results Basak et al. [6], Pr and Gr have been considered as 0.7 and 10^4, respectively. $1 < Re < 100$ has also been changed.

Figures 3 and 4 Present stream function and temperature contour in comparison with Basak et al. [6]. The acceptable harmony among figures and their results validates the accuracy of this study.

Table 4 Some meshes used for solving the problem

Ri	**Standard k-ε**			**RNG k-ε**			**RSM**		
Ri = 0.1	50 × 50	100 × 100	175 × 175	50 × 50	150 × 150	200 × 200	75 × 75	150 × 150	225 × 225
Ri = 1	75 × 75	125 × 125	200 × 200	75 × 75	175 × 175	250 × 250	100 × 100	175 × 175	275 × 275
Ri = 10	100 × 100	150 × 150	225 × 225	100 × 100	200 × 200	300 × 300	125 × 125	200 × 200	350 × 350

Table 5 Details of the Rectangular and Square Enclosures

	Tian and Karayiannis [14], Ampofo and Karayiannis [15], Peng and Davidson [16], Omri and Galanis [17] and Hsieh and Lien [18]	**Betts and Bokhari [19] and Hsieh and Lien [18]**
Rayleigh Number	1.58×10^9	1.43×10^6
Length of Enclosure (m)	0.75	2.18
Wide of Enclosure (m)	0.75	0.076
Left Wall Temperature (°C)	50	15.6
Right Wall Temperature (°C)	10	54.7
Prandtl Number	0.707	0.697

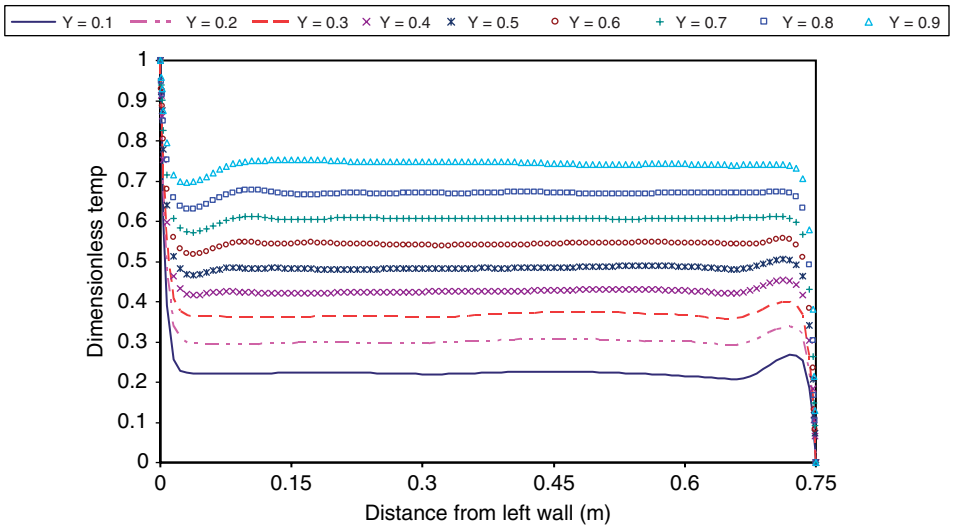

Figure 1 Temperature distribution at different height, in comparison with Tian and Karayiannis [14], Omri and Galanis [17] and Hsieh and Lien [18].

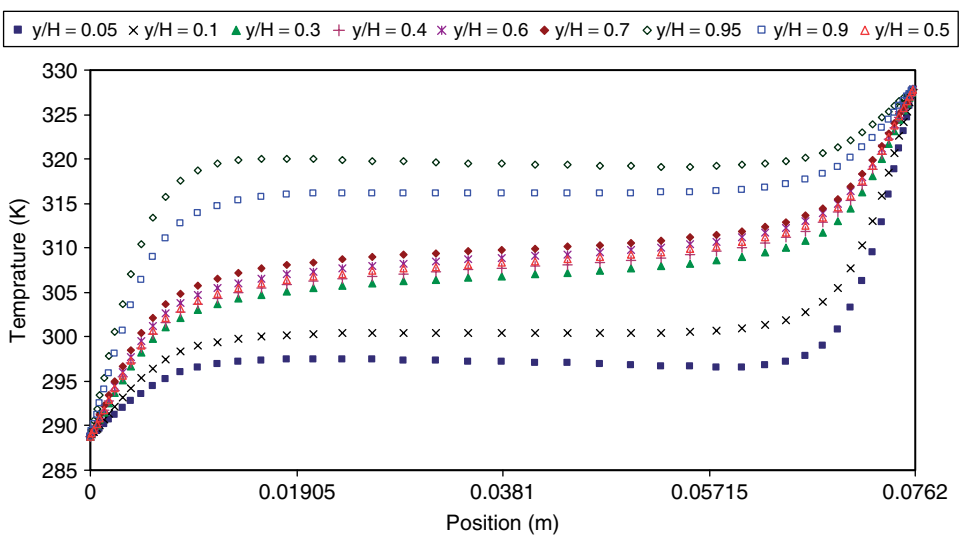

Figure 2 Variation of temperature in $Ra = 1.43 \times 10^6$, in comparison with Betts and Bokhari [19].

3.4. EVALUATION OF TURBULENT MIXED CONVECTION FLOW INSIDE A SQUARE ENCLOSURE

Figure 5 shows the schematics of the problem. In this case, Richardson Number varies from 0.1 to 10.

3.4.1. Validation

Figures 6 and 7 demonstrate some instances of y^+ curve resulted from the present study. The study of these curves reveals the accuracy of mesh that created in boundary layer inside the enclosure.

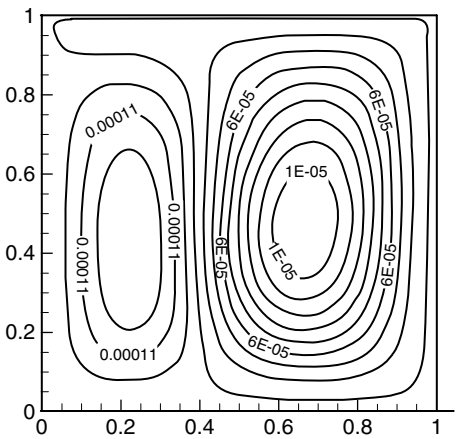

Figure 3 Stream Function with Re = 10, in comparison with Basak et al. [6].

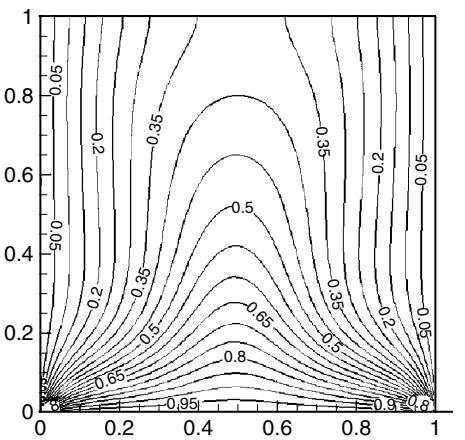

Figure 4 Temperature Contour with Re = 1, in comparison with Basak et al. [6].

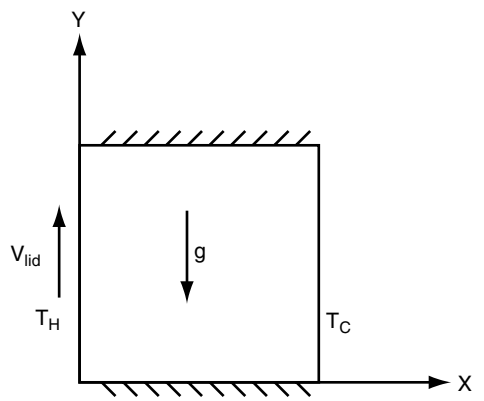

Figure 5 Schematic of the problem.

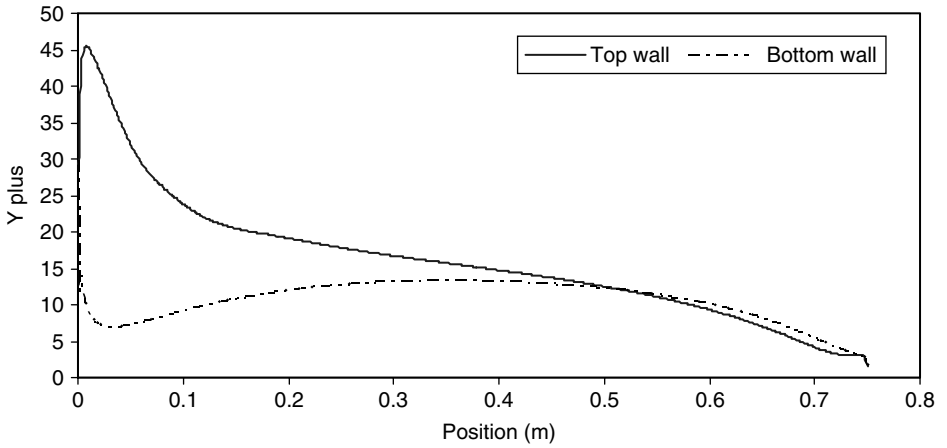

Figure 6 y^+ Diagram on Upper and Lower Walls.

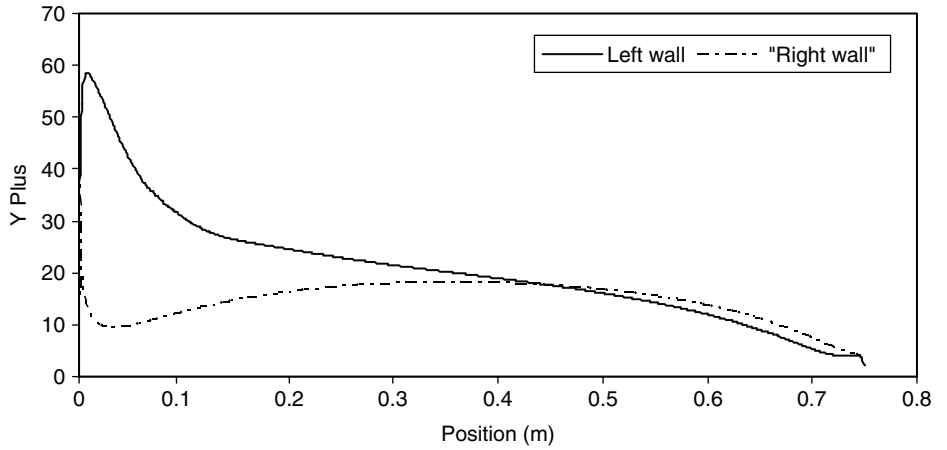

Figure 7 y^+ Diagram on Left and Right Walls.

Figure 8 shows the vertical velocity along the med height for different turbulent and Richardson Numbers. For Ri = 10, it s clear that the velocity on the left wall is maximum. At boundary layer region, flow has a quick haste and thereby the velocity declines increasingly. Upon the exit from the boundary layer, the velocity takes a more or less straight line until the vicinity of the right wall where it reaches the cold wall boundary layer. There again the flow takes on substantial amount of haste and hence deviates with a sharp gradient and declines. At Ri = 0.1 where the vertical velocity has a undeniable role in the flow, The vertical velocity is maximum on the moving wall and it declines with a pretty much even haste as we go from the moving wall to the fixed right wall. This happens in a way that it assumes negative values on the right hand side of the enclosure. At Ri = 1 which symbolizes the predominance of both natural and forced convection at the same time, V behaves the same way as in Ri = 0.1. But the gradient at this state has more tendencies towards Zero than towards negative values. So it can be inferred that the state of V at Ri = 1 is something in between its state at Ri = 0.1 and Ri = 10.

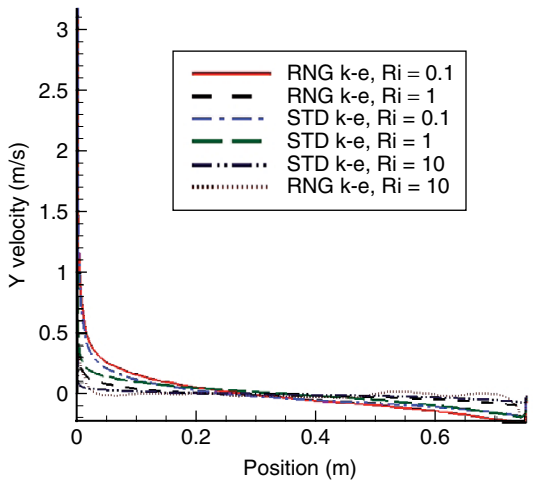

Figure 8 Vertical Velocity at y/H = 0.5.

Figure 9 shows the Nusselt Number diagram on hot wall at different Richardson Numbers. As a result of this figure, it s clear that the Nusselt Number is maximum for the case of Ri = 0.1 and its moderately decrease due to increase of value of Ri. According to the determination of Richardson Number, this means that for Ri = 0.1, the forced convection governs on fluid treatment. So the rate of heat transfer from enclosure increased as a result of lessens Richardson Number. Moreover, the rate of heat transfer by natural convection will be growth; if the Richardson Number will be increment. In large Richardson Numbers, the natural convection is a major parameter of heat transfer in a enclosure. Although, this figure demonstrates that the rate of heat transfer by mix and forced convection is much more than natural convection.

Figures 10 to 13 are Reynolds stress graphs for RSM turbulent model and along the height median. It is inferred from the graphs that the value of UU Reynolds stress is very close to that of VV Reynolds stress. Also the change pattern in all UU, VV and WW Reynolds stress graphs are similar. But the values of WW Reynolds stress are approximately 1.48 times the value of UU and VV stresses.

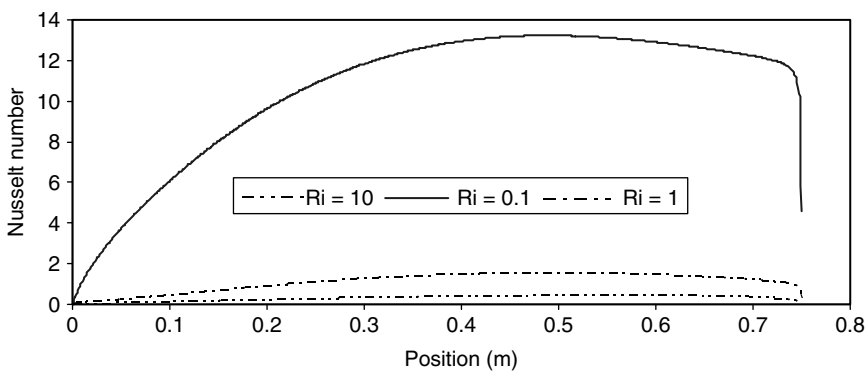

Figure 9 Nusselt Number along the Hot Wall.

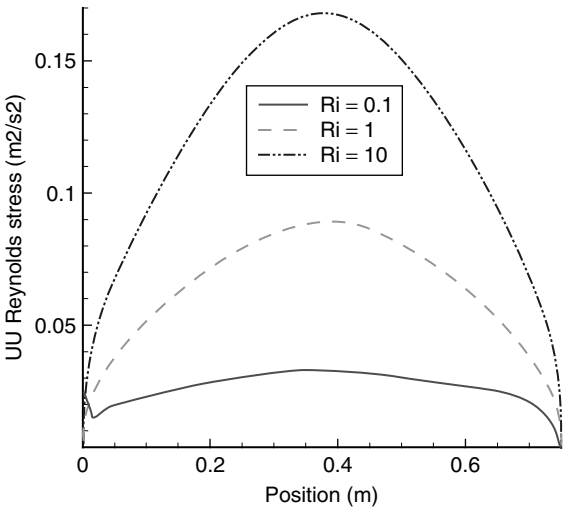

Figure 10 UU Reynolds Stress Diagram at y/H = 0.5.

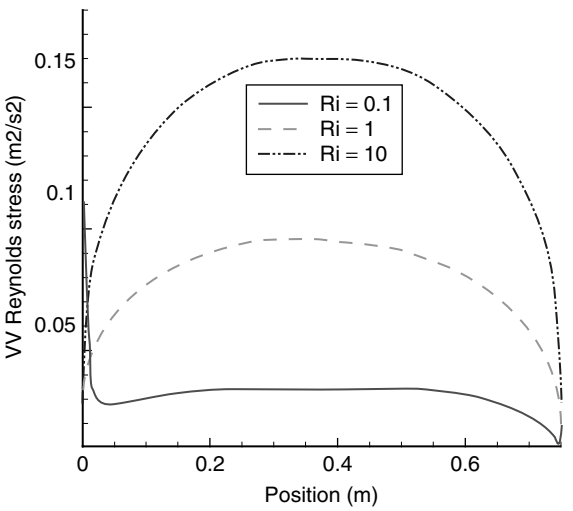

Figure 11 VV Reynolds Stress Diagram at y/H = 0.5.

The UV stress assume values 10 times smaller than values of UU, VV and WW Reynolds stresses (UV~O (10^{-1})). Also UU, VV and WW stresses assume the maximum values at Ri = 10 and minimum values at Ri = 0.1. But for the UV stress, the reverse is the case. It s meaning that maximum values occur for forced convection governing and the minimum values occur when free convection is governs on the flow. Also as the existing graphs and curves for the mentioned stress show, the UU, VV and WW Reynolds stress take zero value on the walls and take maximum value at the center of the enclosure. The UV stress has large values on the left wall. From There after they increase up to a peak at the end of inner layer. Then decrease almost down to x/H = 0.4~0.47 and afterwards increase again almost up to

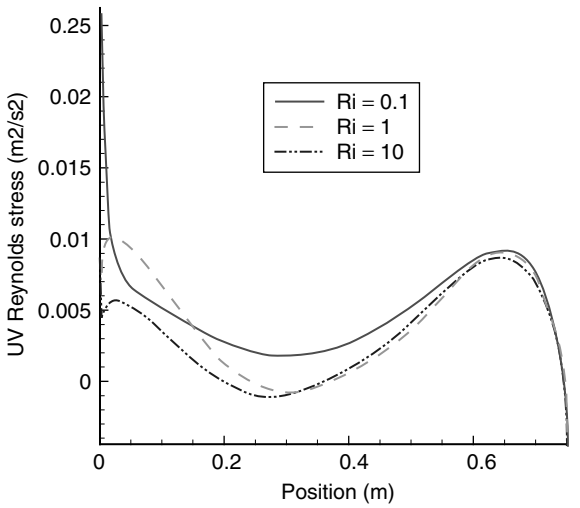

Figure 12 UV Reynolds Stress Diagram at y/H = 0.5.

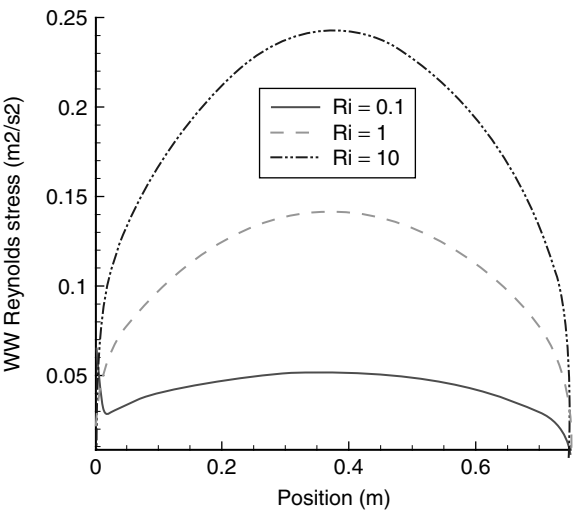

Figure 13 WW Reynolds Stress Diagram at y/H = 0.5.

x/H~0.86. There, The UV stress decline on value due to proximity to the right wall until take negative values on the wall itself.

Figures 14 to 16 show contours of stream functions at different Richardson Numbers. It is obvious that at Ri = 0.1, because of the strong presence of an inertia force related to the velocity of the left wall which is surmounted on buoyancy force inside the enclosure, the entire flow tends towards the left wall particularly the upper part where flow exits the enclosure. At Ri = 1 the balance between the inertia and buoyancy force reduces the flow s tendency towards the moving wall. At Ri = 10 buoyancy force has defeated the inertia force causing the stream function to adopt a symmetrical recirculation shape. The above contour basically

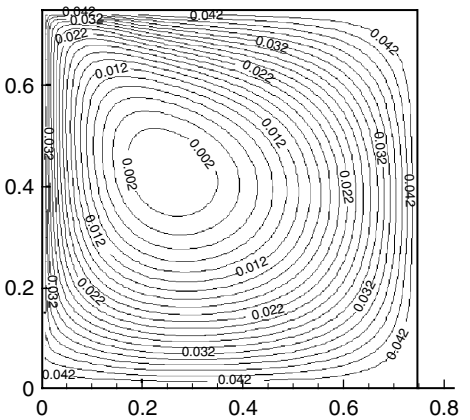

Figure 14 Contour of Stream function at Ri = 0.1.

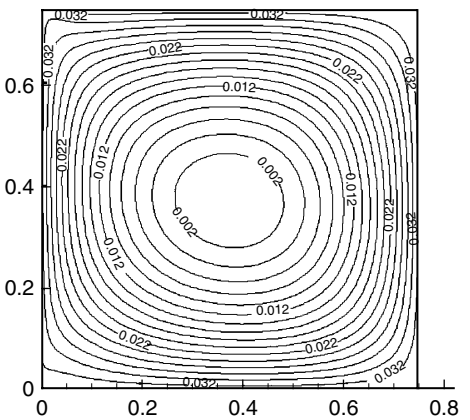

Figure 15 Contour of Stream function at Ri = 1.

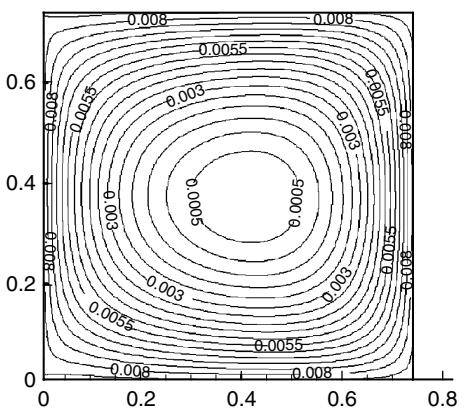

Figure 16 Contour of Stream function at Ri = 10.

shows that the stream function at the center of enclosure is ten times smaller than near the horizontal insulating wall. This implies that the flow is rather stationary at the center of the enclosure.

Figure 17 represents turbulent kinetic energy contour at Ri = 10 for RNG $k-\varepsilon$ Turbulent model. Similar to the contour proposed in Omri and Galanis [17] paper, it is understood from this contour that at free convection, the turbulence is important in the upper part of the hot wall (left wall) and in the lower part of the cold wall (right wall). It is also inferred from this contour that the horizontal adiabatic walls tend to the flow along the horizontal wall keep laminar. Also these walls try to make the flow along the vertical walls and in the beginning of the increasing region and at the end of decreasing region laminar.

As such, the turbulence increases near the hot wall between y/H = 0.2 and y/H = 0.5 and then decreases slightly between y/H = 0.5 and y/H = 0.8 as we approach to horizontal walls. A similar explanation is valid at the vicinity of the cold wall. The kinetic energy profile demonstrates a perfect symmetry at Y/H = 0.5 but this symmetry does not happen at other Y/Hs.

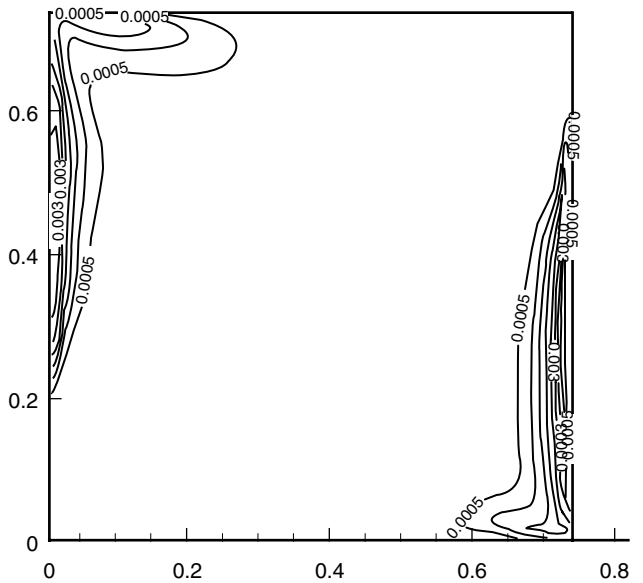

Figure 17 Contour of Turbulent Kinetic Energy at Ri = 10.

4. CONCLUSIONS

In this study, Turbulence mixed convection in air filled enclosures was Modeling Numerically by Standard $k-\varepsilon$, RNG $k-\varepsilon$ and RSM turbulence models for different Richardson Numbers. The governing equations have been solved to small reminders using finite volume method. The results show that:

- In large Richardson Numbers, the natural convection is a major parameter of heat transfer in an enclosure.
- The rate of heat transfer by mix and forced convection is much more than natural convection.

- At high Richardson Numbers, Turbulent kinetic energy profile demonstrates a perfect symmetry at Y/H = 0.5 but this symmetry does not happen at other Y/Hs.
- When Natural convection governs on the flow, the flow is rather stationary at the center of the enclosure.
- At all Richardson Numbers, The UV stress assumes values 10 times smaller than values of UU, VV and WW Reynolds stresses.
- For the UV stress, Maximum values occur for forced convection governing and the minimum values occur when free convection is governs on the flow.

REFERENCES

[1] Bejan A., *Convection heat transfer*, A Wiley-Interscience publication, John Wiley, New York, 2004.

[2] Rahman M. M., Alim M. A., Mamun M. A. H. and et al., Numerical Study of Opposing Mixed Convection in a Vented Enclosure, *ARPN Journal of Engineering and Applied Sciences*, 2007, Vol. **2**, 25–35.

[3] Saha S., M. Ali and et al., Combined Free and Forced Convection inside a Two-Dimensional Multiple Ventilated Rectangular Enclosure, *ARPN Journal of Engineering and Applied Sciences*, 2006, Vol. **1**, 23–35.

[4] Saha S., Mamun A. H., Hossain M. Z. and et al., Mixed Convection in an Enclosure with Different Inlet and Exit Configurations, *Journal of Applied Fluid Mechanics*, 2008, Vol. **1**, 78–93.

[5] Ghasemi B. and Aminossadati S. M., Natural Convection Heat Transfer in an Inclined Enclosure Filled with a Water-CuO Nanofluid, *Numerical Heat Transfer: Part A*, 2009, Vol. **55**, 807–823.

[6] Basak T., Roy S., Sharma P. K. and et al., Analysis of Mixed Convection Flows within a Square Cavity with Uniform and Non-Uniform Heating of Bottom Wall, *International Journal of Thermal Sciences*, 2009, Vol. **48(5)**, 891–912.

[7] Khanafer K.M., Al-Amiri A. M. and Pop I., Numerical Simulation of Unsteady Mixed Convection in a Driven Cavity Using an Externally Excited Sliding Lid, *European Journal of Mechanics B: Fluids*, 2007, Vol. **26**, 669–687.

[8] Goshayeshi H. R. and Safaei M. R., Investigation of turbulence mixed convection in air-filled enclosures, *Journal of Chemical Engineering and Materials Science*, 2011, Vol. **2(6)**, 87–95.

[9] Bessaih R. and Kadja M., Turbulent natural convection cooling of electronic components mounted on a vertical channel, *Applied Thermal Engineering*, 2000, Vol. **20**, 141–154.

[10] Ampofo F., Turbulent natural convection in an air filled partitioned square cavity, *International Journal of Heat and Fluid Flow*, 2004, Vol. 25, 103–114.

[11] Salat J., Xin S., Joubert P. and et al., Experimental and numerical investigation of turbulent natural convection in a large air-filled cavity, *International Journal of Heat and Fluid Flow*, 2004, Vol. **25**, 824–832.

[12] Xaman J., Alvarez G., Lira L. and et al., Numerical study of heat transfer by laminar and turbulent natural convection in tall cavities of facade elements, *Energy and Buildings*, 2005, Vol. **37**, 787–794.

[13] Aounallah M., Addad Y., Benhamadouche S. and et al., Numerical investigation of turbulent natural convection in an inclined square cavity with a hot wavy wall, *International Journal of Heat and Mass Transfer*, 2007, Vol. **50**, 1683–1693.

[14] Tian Y. S. and Karayiannis T. G., Low Turbulence Natural Convection in an Air Filled Square Cavity, *International Journal of Heat and Mass Transfer*, 2000, Vol. **43**, 849–866.

[15] Ampofo, F. and Karayiannis, T. G., Experimental benchmark data for turbulent natural convection in an air filled square cavity, *International Journal of Heat and Mass Transfer*, 2003, Vol. **46**, 3551–3572.

[16] Peng S. H. and Davidson L., Large Eddy Simulation for Turbulent Buoyant Flow in a confined cavity, *International Journal of Heat and Fluid Flow*, 2001, Vol. **22**, 323–331.

[17] Omri M. and Galanis Ni., Numerical analysis of turbulent buoyant flows in enclosures: Influence of grid and boundary conditions, *International Journal of Thermal Sciences*, 2007, Vol. **46**, 727–738.

[18] Hsieh K. J. and Lien F. S., Numerical Modeling of Buoyancy-Driven Turbulent Flows Enclosures, *International Journal of Heat and Fluid Flow*, 2004, Vol. **25**, 659–670.

[19] Betts P. L. and Bokhari I. H., Experiments On Turbulent Natural Convection In An Enclosed Tall Cavity, *International Journal of Heat and Fluid Flow*, 2000, Vol. **21**, 675–683.

[20] Safaei, M. R., *The Study of Laminar and Turbulence Mixed Convection Heat Transfer in Newtonian and Non-Newtonian Fluids inside Rectangular Enclosures in Different Ri Numbers*, M. Sc. thesis, Azad University-Mashhad Branch, Iran, 2009 (in Farsi Language).

[21] Patankar S. V., *Numerical Heat Transfer and Fluid Flow*, Hemisphere Washington, 1980.

[22] Goshayeshi H. R., Safaei M. R. and Maghmoomi Y., Numerical Simulation of Unsteady Turbulent and Laminar Mixed Convection in Rectangular Enclosure with Hot upper Moving Wall by Finite Volume Method, *The 6th International Chemical Engineering Congress and Exhibition (IChEC 2009)*, Kish Island, Iran, 2009.

NOMENCLATURE

u, v	Velocities in x and y Directions	(m/s)
x, y	Cartesian Coordinates	(m)
P	Pressure	(N/m^2)
T	Temprature	(K)
t	Time	(sec)
g	Gravitational Acceleration	(m^2/s)
K	Turbulent Kinetic Energy Transport	(m^2/s^2)
k	Thermal Conductivity	$(W/m.k)$
Re	Reynolds Number	
Ri	Richardson Number	
Gr	Grashof Number	
Nu	Nusselt Number	
Pr	Prandtl Number	
Ra	Rayleigh Number	
ε	Dissipation of Turbulent Kinetic Energy Transport	(m^2/s^3)
υ_t	Turbulent Kinematic Viscosity	(m^2/s)
σ_T	Turbulent Thermal Diffusivity	(m^2/s)
β	Thermal Expansion Coefficient	(1/K)
ρ	Density	(kg/m^3)
υ	Kinematics Viscosity	(m^2/s)

Subscripts

h	Hot Wall
c	Cold Wall
m	Mean
lid	Lid